JOURNAL OF MATERIALS SCIENCE 29 (1994) 39–46

Environmental stress cracking of PVC and PVC-CPE

Part II *Failure mechanisms*

J. BREEN
TNO Plastics and Rubber Research Institute, P.O. Box 6031, 2600 JA Delft, The Netherlands

The failure of unnotched PVC and PVC-CPE was studied in a number of vapour and liquid environments. The failure mechanisms observed are related to craze initiation and logarithmic craze growth. A model to explain the origin of the logarithmic craze growth is presented. The failure mechanism in air and in benzene and toluene vapours is ductile, whereas it is brittle in *n*-hexane, *n*-decane and ethanol vapours, *n*-octane/benzene mixtures and natural gas condensate. Equations to describe the time to failure for both failure mechanisms are derived. The ductile failure is ascribed to plasticization and/or plastic deformation around the craze. Brittle failure is thought to arise from crazes which reach a critical size.

1. Introduction

Environmental stress cracking of PVC (polyvinylchloride) and PVC-CPE (chlorinated polyethylene modified PVC) materials in vapours and liquids has been studied in order to predict the lifetime of the PVC and PVC-CPE gas pipes used for the low pressure gas distribution system in the Netherlands. Although the environmental stress cracking of PVC and PVC-CPE by *n*-alkane and/or benzene enriched natural gas environments can be attributed to a physical action which results in an accelerated crazing [1], the correlation between the craze initiation stress and the failure stress is not obvious. In a previous paper [2], it was shown that the long-term craze initiation stress of PVC and PVC-CPE in benzene enriched natural gas vapours was significantly lower than the corresponding long-term failure stress. This phenomenon was associated with the cessation of the craze growth.

The decrease of the craze initiation stress as a function of the environment was modelled in the first paper of this series [1]. This paper focuses on the surface craze growth and the failure mechanisms of PVC and PVC-CPE in environments with physical stress cracking capacities. Special attention is payed to the cessation and the renewal of craze growth. Simple models are presented to describe the experimental failure curves.

The failure curves of unnotched polymer specimens in liquids under a constant loading show three zones [3, 4]. At high stress levels, a behaviour similar to that in the absence of the liquid is observed. At intermediate stress levels, a steep decrease in failure stress within a short time interval is found. This phenomenon is ascribed to the penetration of liquid in the growing crack [4]. At low stress levels the failure stress hardly decreases with the time of loading. The latter case is called "pure" environmental stress cracking by Shanahan *et al.* [4]. The so-called pure environmental stress cracking will determine the long-term failure stress. However, to predict the long-term failure stress, insight into the failure mechanisms responsible for the rupture at intermediate stress levels is needed.

An analogous three zones failure behaviour is observed for notched specimens [5], where a plot of stress intensity versus crack growth rate is used to describe the failure process. The stress intensity is proportional to the stress and the crack growth rate is inversely proportional to the time to failure. Williams and Marshall explained the failure behaviour in the high stress zone and the low stress zone by relaxation processes typical for, respectively, the original and the plasticized polymer matrix at the crack tip [6]. The failure process at intermediate stress levels was interpreted by a viscous flow [6].

In this paper it will be argued that the failure process at intermediate stress levels in unnotched specimens is caused by craze-growth. The failure behaviour of notched PVC and PVC-CPE specimens in environments will be presented in a forthcoming paper of this series.

2. Theory

In order to predict the failure curve in environments which lead to an accelerated craze initiation, knowledge about craze growth under these circumstances is essential. From experimental results it is concluded that the development of crazes will affect the time to failure of a stressed polymer product. In this section the current and an alternative model for craze growth will be presented.

A well-developed model for craze growth is based upon the meniscus instability which occurs, e.g. in a

0022–2461

viscous fluid between two parallel plates under the action of a pressure gradient [7, 8]. This model leads to a linear craze growth rate which depends on the thickness of the deformed zone (craze), the applied stress and a number of constants of the material under study. The meniscus instability model can be applied to both the fast and the slow craze growth. The fast craze growth corresponds to the situation in which the penetration of the aggressive medium is slow compared to the craze growth, whereas the slow craze growth corresponds to the situation in which the penetration of the aggressive medium is fast compared to the craze growth. When the penetration of the environment into the polymer matrix at the craze tip interferes with the craze growth, the (capillary) pressure gradient over the craze becomes the driving force. This means the longer the craze, the slower the craze growth. The craze length then scales with the square root of the time of exposure.

Although the meniscus instability model seems to be adequate for notched test samples, it fails to describe the experimental results on surface crazes in unnotched PVC and PVC-CPE in the environments studied. The constant stress distribution at the craze tip assumed in the meniscus instability model seems not to be appropriate. A model in which the viscoelastic behaviour of the polymeric material, the influence of neighbouring crazes, the kinetic contribution, the elastic contribution and the plastic contribution during craze growth is incorporated was formulated by Zhang *et al.* [9]. However, this model can only be applied to the surface crazes observed in PVC and PVC-CPE when the different contributions can be quantified.

2.1. Simple model for craze growth

Here a more simply model for craze growth is preferred [10]. This model is based partly on the same arguments as the one on logarithmic craze growth by Heymans *et al.* [11]. During the growth of a craze with a constant thickness under an applied stress σ, a proportion holds for the release rate of elastic energy dU_{el}/dt:

$$\frac{dU_{el}}{dt} \propto \frac{\sigma^2}{E}\frac{da}{dt} \tag{1}$$

where E is the modulus of the material under study and da/dt the craze growth rate (a = craze length). Because of the strain softening showed by PVC and PVC-CPE, it is assumed that the release of elastic energy is almost completely consumed by the plastic deformation in a small volume element at the tip of the craze. The relation for the dissipation rate of plastic energy dU_{pl}/dt then becomes:

$$\frac{dU_{pl}}{dt} \propto \sigma_{pl}\frac{d\varepsilon}{dt} \tag{2}$$

where σ_{pl} is the cold drawing stress and $d\varepsilon/dt$ the straining rate in the small energy consuming element at the craze tip. Instead of an analysis of the straining rate according to a non-Newtonian fluid, here an analysis according to a thermoactivated process is preferred. The relation for the straining rate then becomes [12]:

$$\frac{d\varepsilon}{dt} \propto \exp(\gamma\sigma_{pl}/k_B T) \tag{3}$$

where γ is an activation volume, k_B Boltzmann's constant and T the temperature in K. The time dependence of the drawing stress leading to plastic deformation can be approximated by:

$$\sigma_{pl} = A - \frac{k_B T}{\gamma}\ln t \tag{4}$$

where A is a constant ($A \gg k_B T/\gamma$) and t the time to plastic deformation. Substitution of Equation 4 into Equation 3 shows that $d\varepsilon/dt$ is inversely proportional to the loading time, The proportion of Equation 2 then reduces to:

$$\frac{dU_{pl}}{dt} \propto \frac{\sigma_{pl}}{t} \tag{5}$$

Because it is assumed that the release rate of elastic energy almost equals the dissipation rate of plastic energy, the relation for craze growth become:

$$\frac{da}{dt} \propto \frac{\sigma_{pl}E}{\sigma^2}\frac{1}{t} \tag{6}$$

Neglect of the time dependence of the cold drawing stress, σ_{pl}, and the modulus, E, results in:

$$\frac{da}{d\ln t} = \text{constant} \tag{7}$$

the condition for logarithmic craze-growth. From Equation 6 it is concluded that the initial craze growth is inversely proportional to the loading time needed for craze initiation. For loading times less than the time to craze initiation, the relation for the craze growth has of course no validity. Thus the equations for craze growth only apply for stress levels exceeding the threshold stress for craze initiation.

The cessation of craze growth is thought to be caused by crack shielding [13], i.e. by the decrease of the stress at the craze tip as a function of the loading time. Crack shielding is caused by local flow and hence is related to polymer segment mobility.

2.2. Relation between craze growth and time to failure

The growth of surface crazes and the time to failure cannot be correlated directly to these phenomena in notched test specimens which fail by craze and crack growth [14]. In the next paper of this series, the failure of notched specimens will be treated. Here two failure mechanisms are considered: (1) failure by cold drawing of the intact ligament of the cross-section containing the largest crazes; (2) failure induced by craze/crack instability.

2.2.1. Ductile failure

The first failure mechanism neglects the stress concentration at the craze tip. This is allowed for situations

where the plastically deformed zone in front of the craze tip is large. Failure is thought to occur as soon as the stress in the intact ligament exceeds the stress for cold drawing. The stress for cold drawing decreases with loading time. The relation between the stress for cold drawing and the time to failure is presented in Equation 4. In a cross-section where crazes develop, the net stress in the intact ligament will increase by craze growth and/or by a decrease in the load carried by the craze fibrils. An integral equation has to be solved in order to obtain the time to failure:

$$1 = \frac{1}{t_\infty}\exp -(U_{act}/k_B T)\int_0^{t_f} \exp[\sigma_1(t)\,\gamma/k_B T]\,dt \quad (8)$$

where U_{act} is the activation energy for the cold drawing, k_B Boltzmann's constant, T the absolute temperature, γ the activation volume, $\sigma_1(t)$ the stress in the intact ligament, t_∞ a constant and t_f the time to failure. If the stress over the craze is $\sigma_c(t)$ and the stress concentration at the craze tip is neglected, the net stress in the intact ligament is given by:

$$\sigma_1(t) = \frac{\sigma_a - r(t)\sigma_c(t)}{1 - r(t)} \quad (9)$$

where σ_a presents the applied stress, $r(t)$ the crazed fraction in the cross-section and $\sigma_c(t)$ the stress carried by the craze fibrils.

2.2.2. Brittle failure

The calculation of the time to failure for the second failure mechanism is based on a fracture mechanics criterion. Failure is thought to occur after a critical stress intensity is reached at the craze tip. The stress intensity at the craze tip is a function of the shape of the craze [15] and the size of the active zone around the craze. The active zone is the zone in which the polymer material is deformed plastically. The stress intensity at the craze tip will decrease with increasing thickness of the active zone. Furthermore, the stress intensity at the craze tip is modified by the load carrying capacity of the crazes and by craze fibril breakdown. Here the time to failure is calculated for the most severe situation, namely the situation where the craze is considered to be a crack. The failure criterion then becomes [16]:

$$a(t_f) = 500\,\pi\left(\frac{K_{Ic}}{\sigma_a}\right)^2 \quad (10)$$

where a represents the craze length in mm, t_f the time to failure, σ_a the applied stress in MPa and K_{Ic} the critical stress intensity factor in MPa m$^{1/2}$.

3. Experimental procedure

The PVC and PVC-CPE materials used in this study are described elsewhere [2]. The chemicals used were of analytical grade. All experiments were performed at 23 °C. The creep experiments were performed on tapered test strips [2]. These test strips were also used for craze growth experiments. The experimental procedures for the creep test and the craze growth measurement have been described by Wales [17]. The determination of the time to failure was performed on dumb-bell shaped test strips [2]. The equipment used for these test strips was described in the same paper.

4. Results

Some craze growth results have been presented earlier [17]. In Fig. 1 the results of the logarithmic craze growth rate are presented for surface crazes in PVC at 23 °C in natural gas enriched benzene (50% relative saturation). The curve shown in this figure represents the fit of the maximum logarithmic craze growth rate observed in PVC in air at 23 °C. This fit was based on a logarithmic craze growth rate which is inversely proportional to the square of the applied stress (see Equation 6). The dashed curve shown in Fig. 1 also seems to hold for the maximum craze growth rate observed in a benzene enriched natural gas environment. Craze growth measurements performed in other environments studied lead to the same conclusion. Therefore an environment independent maximum craze growth rate for PVC as a function of the applied stress can be defined:

$$\beta = \frac{da}{d\ln t} = \frac{59}{\sigma^2}\,(\text{mm}) \quad (11)$$

where the applied stress σ has to be expressed in MPa.

The enormous scatter in the craze growth rate of individual crazes can be attributed to a number of reasons, e.g. distribution of surface inhomogeneities, scratches and the viscoelastic behaviour of the polymer. Those crazes showing the maximum logarithmic craze growth rate are most suspect as initiating the ultimate failure process. Therefore these crazes will be dealt with in the calculation of the failure curve (see Discussion).

Craze growth stops or is reduced greatly after a certain period. The strongly reduced craze growth process observed after this period is probably caused by significant creep on a scale large compared to the craze thickness. When cessation of craze growth occurs, the period of craze growth between craze initia-

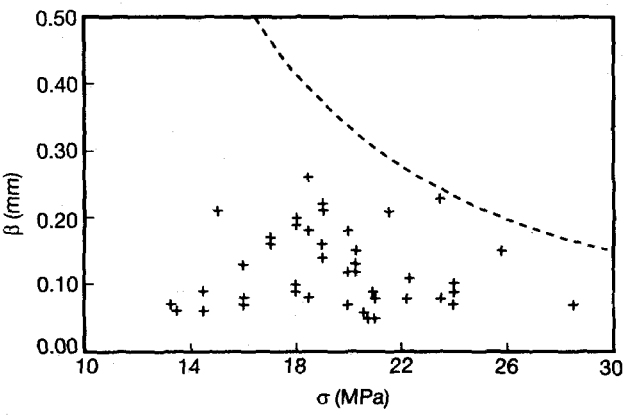

Figure 1 Logarithmic craze growth rates, $\beta = da/d\log t$, for surface crazes versus the applied stress. Material: PVC; temperature: 23 °C; environment: benzene (60 000 p.p.m.)–enriched natural gas. The dashed line represents Equation 11 ($d\ln t = 2.3\,d\log t$).

tion and cessation seems to be almost constant on a logarithmic time scale. This means that the cessation of craze growth (the craze shielding) and the craze initiation are related. A sound explanation for this phenomenon is unknown.

To complicate the craze growth process even more, a renewal of craze growth after cessation or a continuous craze growth is observed in a number of environments, e.g. in ethanol and *n*-hexane vapour a renewal of craze growth is found at stress levels exceeding the craze initiation stress. This renewal is accompanied by crack growth and results in a relatively fast failure of the test strip. The crack growth and the failure of the test strip results in an elongation of the test strip. This elongation is represented as a strain in Fig. 2. The short-term strain observed scales with the applied stress, as is expected for an elastic material. The craze initiation and the initial craze growth hardly seem to affect the overall creep behaviour of the test strip. In air, an onset of curvature is observed at about 10^5 s, which is not due to the initiation or growth of crazes but due to the start of necking in the test strip. The onset of curvatures observed for the PVC-CPE test strip in toluene vapour has to be attributed to plasticization, since in toluene the PVC-CPE material becomes rubbery.

The renewal of the craze growth is hard to follow by craze growth measurements, because the renewal of craze growth seems to occur simultaneously for many crazes. Craze bands are formed, which do not allow individual crazes to be studied. These craze bands can be observed in Fig. 3. It shows the failure of a PVC-CPE test strip in natural gas enriched with *n*-octane (50% relative saturation) under 30 MPa at 23 °C.

The renewal of the craze growth is not limited to growth at the surface, as can be noticed from Fig. 4. In Fig. 4 a SEM (scanning electron microscope) micrograph of the fracture surface of a PVC-CPE test strip

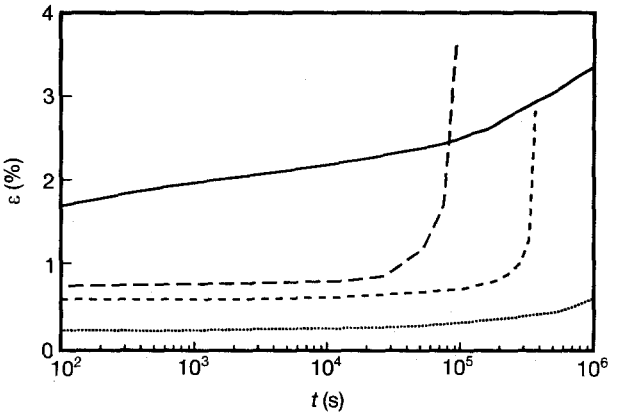

Figure 2 Strain of PVC-CPE test strips as a function of the loading time in air and in vapours under different stress levels. Temperature: 23 °C. ——— air, σ = 30 MPa; — — saturated *n*-hexane vapour, σ = 12 MPa; – – – saturated ethanol vapour σ = 15 MPa; ..... saturated toluene vapour, σ = 8.6 MPa.

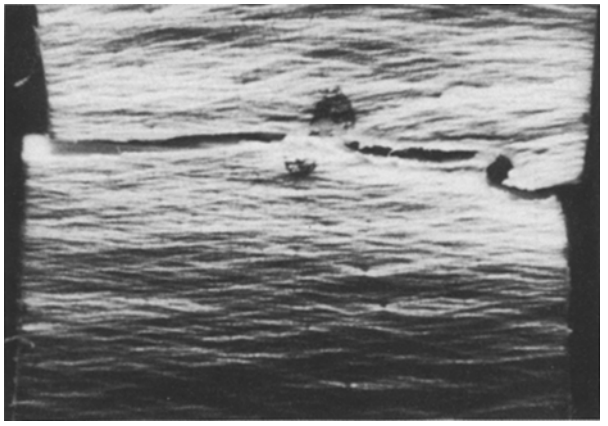

Figure 3 Failure of a loaded PVC-CPE test strip after renewal of craze growth (craze yielding). Environment: *n*-octane (50% relative saturation); stress level: 32 MPa; temperature: 23 °C.

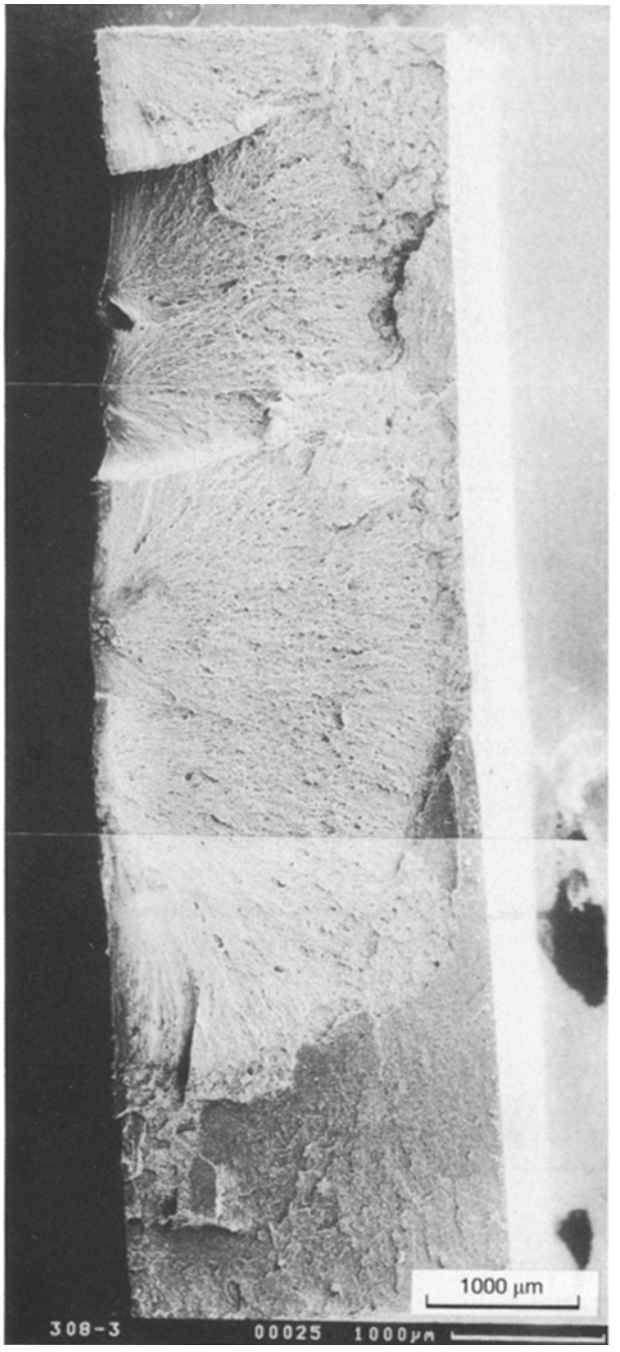

Figure 4 SEM micrograph of a PVC-CPE fracture surface. Environment: *n*-octane (50% relative saturation); stress level: 27 MPa; temperature: 23 °C; magnification: 25 ×.

is shown. This test strip broke in natural gas enriched with *n*-octane (50% relative saturation) under a stress of 27 MPa at 23 °C as a result of a renewal of craze growth. The direction of the craze growth is revealed by the orientation of the broken fibrils (white zones). After the craze reached the opposite side of the test strip, the failure process most probably became unstable, as can be concluded from the dark lower part of the surface. In this dark lower part, melt phenomena were observed at higher magnifications.

The rather brittle failure which is observed visually for PVC and PVC-CPE stressed in, for example, ethanol, *n*-hexane and natural gas enriched with *n*-alkanes is less dramatic than it appears. The stress interval in which this brittle failure process occurs is rather narrow, as is shown in Fig. 5 for PVC-CPE in natural gas enriched with *n*-decane. The failure stress of PVC-CPE in natural gas enriched with *n*-decane decreases moderately compared to the one in air. The threshold value of the failure stress of PVC-CPE in the *n*-decane enriched natural gas environment seems to equal the long term craze initiation stress [1].

A stronger decrease in failure stress is observed for the stressed PVC and PVC-CPE test strips exposed to *n*-octane/benzene mixtures (see Fig. 6). This stronger

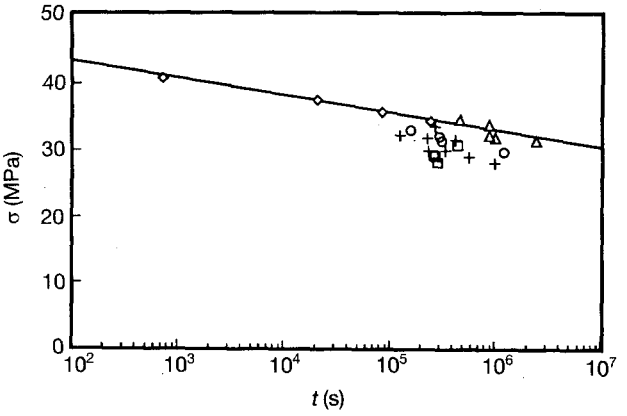

Figure 5 Stress versus time to failure for PVC-CPE in air and in *n*-decane enriched vapours. Temperature: 23 °C. ◇ air; △ 12.5; ○ 25; + 50; □ 80% relative saturation of *n*-decane. The solid line represents ductile failure of PVC-CPE in air.

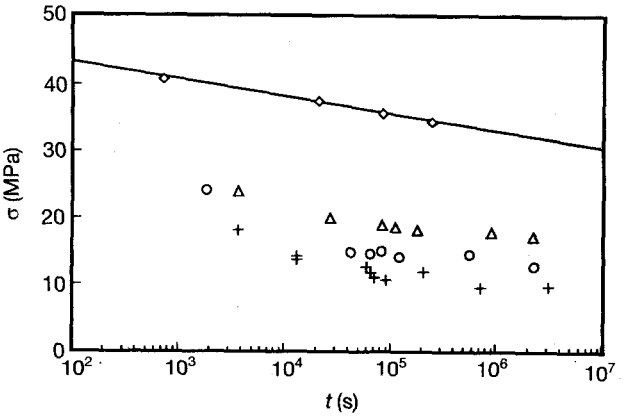

Figure 6 Stress versus time to failure for PVC-CPE in air and in *n*-octane/benzene mixtures. Temperature: 23 °C. ◇ air; △ 100; ○ 90; + 80% *n*-octane. The solid line represents ductile failure of PVC-CPE in air.

decrease can be related to a lower long-term craze initiation stress [1]. The failure mechanism of PVC and PVC-CPE in these environments again is determined by renewal or acceleration of craze growth and the threshold value of the failure stress seems to equal the long-term craze initiation stress.

In benzene enriched natural gas vapours [2] on the other hand, the long-term failure stress does not seem to be related to the craze initiation stress. The brittle failure observed for stressed PVC and PVC-CPE in the *n*-octane/benzene mixtures and the ductile failure observed in benzene vapours are considered to represent the extreme failure mechanisms for PVC and PVC–CPE in aggressive (physical interactions only) environments. An intermediate failure mechanism is expected in situations where the ductile failure competes with the brittle failure. The brittle and ductile failure mechanisms will be modelled and discussed in the next section.

5. Discussion

In modelling environmental craze growth starting from the meniscus instability model, Brown [18] considered two regimes: (1) craze growth fast compared to sorption; (2) craze growth slow compared to sorption. Only the first regime seems to result in craze growth in the PVC materials studied. The transition from the first to the second regime is thought to contribute to the cessation of craze growth in PVC and PVC-CPE. Brittle failure will occur if the transition from the first to the second regime is slow compared to the actual craze growth. A critical craze size is then reached before the transition.

The results presented by Brown cannot be applied to the experimental data given here, because the viscoelastic behaviour of the polymer matrix is neglected in the meniscus instability model. The constant growth rate predicted by the meniscus instability model is a consequence of this neglect.

In the previous section it was shown that crazing plays an important role in the brittle failure of PVC and PVC–CPE in aggressive environments. Crazing seems to be, however, less dominant in the ductile fracture of PVC and PVC-CPE. The ductile failure of PVC-CPE in benzene vapour (50% relative saturation) and the brittle failure of PVC-CPE in natural gas condensate will now be considered in more detail.

5.1. Ductile failure

The effect of crazing in ductile failure can be calculated using Equations 8 and 9. The data points on the ductile failure observed in air at 23 °C are fitted according to Equation 4. In terms of the integral Equation 8, A equals $U_{act} + k_B T \ln t_\infty$. The results of the least squares fits are:

$$\text{PVC-CPE: } \frac{\gamma}{k_B T} = 0.91, \quad \frac{U_{act}}{k_B T} + \ln t_\infty = 44$$

$$\text{PVC: } \frac{\gamma}{k_B T} = 0.80, \quad \frac{U_{act}}{k_B T} + \ln t_\infty = 47$$

The crazed fraction in the cross-section is calculated

starting from the logarithmic craze growth found. It is assumed that the craze growth into the bulk is circular. If n crazes are present in the cross-section which fails, the relation for the crazed fraction r becomes:

$$r(t) = n\frac{\pi}{8}\left(\beta \ln \frac{t}{t_c}\right)^2 \quad (12)$$

where β represents the logarithmic craze growth rate, t_c the craze initiation time, t the actual time and n the number of crazes in the cross-section concerned. The cessation of craze growth is introduced in the following way:

$$r(t) = 0, \quad t \leqslant t_c$$

$$r(t) = n\frac{\pi}{8}\left(\beta \ln \frac{t}{t_c}\right)^2, \quad t_c < t < t_s$$

$$r(t) = n\frac{\pi}{8}\left(\beta \ln \frac{t_s}{t_c}\right)^2, \quad t \geqslant t_s$$

where t_s is the time at which the craze growth stops.

An exponential decay in the stress carried by the craze is assumed:

$$\sigma_c(t) = \sigma_a \exp -(t - t_c/\tau_r) \quad (13)$$

in which σ_a is the stress applied, σ_c the stress carried by the craze, t the actual time, t_c the craze initiation time and τ_r a relaxation time. The relaxation time is thought to depend on the sorption-induced plasticization rate or on the creep rate and is estimated to equal 3×10^5 s in the benzene vapour (50% relative saturation). The square of the logarithmic craze growth times the number of crazes ($n\beta^2$, see Equation 12) is estimated to be about 1/8 mm^2 for the stress interval considered. The product $n\beta^2$ will not vary much within a small stress interval. The increase in the experimental logarithmic craze growth rate with decreasing stress (see Equation 11) is compensated by a decrease in craze density.

The ductile failure mechanism observed for PVC-CPE in benzene vapour (50% relative saturation) is modelled using the experimental craze initiation curve, the cessation of craze growth after 30 times the craze initiation time, the exponential decaying craze stress σ_c (see Equation 13) and the constant $n\beta^2$ value of 1/8 mm^2. The craze initiation curve of PVC-CPE in benzene vapour, the failure curve of PVC-CPE in air and the predicted failure curve of PVC-CPE in benzene vapour are shown in Fig. 7. The predicted failure curve is in agreement with the experimental data.

5.2. Brittle failure

The second failure mechanism which is observed for PVC and PVC-CPE is brittle failure. Brittle failure of stressed PVC and PVC-CPE can be observed in natural gas condensate liquid. However, in agents which cause plasticization, e.g. benzene, embrittlement is also observed at the higher stress levels (short-term experiments). It is believed that embrittlement can be related to the size of the active zone around a craze. If the time to failure is smaller than the sorption time, the active zone will be small and a brittle failure mechanism is expected. The time to failure is calculated according to Equation 10 for brittle failure. The craze is considered to be a crack as far as the stress intensity in front of the craze tip is concerned. Failure will occur after the craze reaches a length which corresponds to the critical stress intensity factor K_{Ic}. The craze length, a, is given by:

$$a = \beta \ln \frac{t}{t_c} \quad (14)$$

in the case of logarithmic craze growth. The logarithmic craze growth rate is quantified by β and the craze initiation time by t_c. The actual time is given by t. Equation 14 is valid for $t > t_c$. Substitution of the empirical relation for the logarithmic craze growth rate, β, (Equation 11) into Equation 14 leads to:

$$a = \frac{59}{\sigma_a^2} \ln \frac{t}{t_c} \quad (15)$$

The relation for the time to failure can be found by

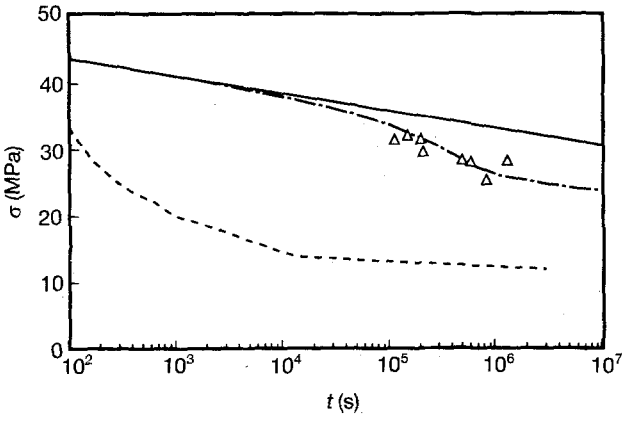

Figure 7 Modelling of the failure data (△) for PVC-CPE in benzene vapour (50% relative saturation). Temperature: 23 °C. ——— ductile failure in air; — — craze initiation curve in benzene vapour; —·— calculated failure curve in benzene vapour [limited logarithmic craze growth ($t_s = 30\ t_c$); exponential decrease in craze loading capacity (see Equation 13; $\tau_r = 3 \times 10^5$ s)].

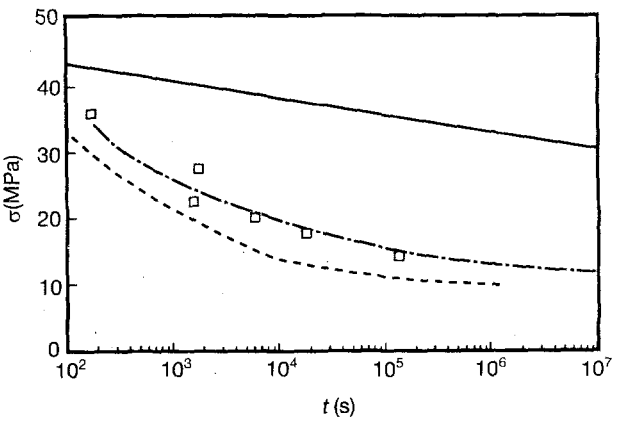

Figure 8 Modelling of the failure data (□) for PVC-CPE in natural gas condensate. Temperature: 23 °C. ——— ductile failure in air; — — craze initiation curve in natural gas condensate; —·— calculated failure curve in natural gas condensate (Equation 16; $K_{Ic} = 0.35$ MPa m$^{1/2}$).

substituting the relation for the length of the craze, a, into Equation 10. The relation for the time to failure, t_f, then becomes:

$$\ln \frac{t_f}{t_c} = 27 K_{Ic}^2 \quad (16)$$

where K_{Ic} represents the critical stress intensity factor in MPa $m^{1/2}$. According to Equation 16, the failure curve can be found by shifting the craze initiation curve horizontally on a logarithmic time scale by a factor of $27\,e^{K_{Ic}^2}$.

The experimental data points for the time to failure of PVC-CPE in natural gas condensate are well described by a critical stress intensity factor of 0.35 MPa $m^{1/2}$. This value of K_{Ic} corresponds to a t_f/t_c value of 27, where t_f is the time to failure and t_c the craze initiation time. The ratio t_s/t_c, where t_s represents the time to cessation of craze growth, amounts to 30–100 in, for example, air and in benzene vapours. Thus, when the processes which decrease and ultimately cease the craze growth are slower than the actual craze growth, brittle failure will occur.

The value of 0.35 MPa $m^{1/2}$ found for K_{Ic} is rather low. The slow crack growth measurements on notched specimens, which are presented in the next paper, yield larger K_{Ic} values. Despite these larger K_{Ic} values, the low K_{Ic} values found here can be explained qualitatively by the differences in shape between a surface craze and a craze in front of a notch.

It is possible to calculate a critical stress intensity factor using Equation 16 from the ratio of the time to failure and the time to craze initiation for every data point. The results are presented in Table I for a number of environments.

It is concluded that brittle failure corresponds to $K_{Ic} < 0.45$ MPa $m^{1/2}$. Furthermore brittle failure is characterized by a ratio t_f/t_c which hardly depends on the stress at failure. When ductile failure is observed, the ratio t_f/t_c increases with decreasing failure stress. The ratio t_f/t_c for PVC-CPE in air is low, because the craze initiation stress is very close to the failure stress in this environment. Macroscopic necking of a PVC-CPE test strip will occur in air before a craze can develop. In benzene vapour the ratio t_f/t_c exceeds 10^3. This ratio can become larger than 10^6 at stress levels close to the threshold craze initiation stress. Craze growth ceases after $t_s/t_c \approx 30$ in this environment, which excludes failure by a continuous craze growth in benzene vapours.

From experimental observations it is concluded that the failure mechanism is brittle for $t_f/t_c < 100$. After cessation of craze growth, brittle failure becomes less probable. The reason for brittle instead of ductile failure is not attributed to a higher craze growth rate, but to a smaller critical stress intensity factor. The magnitude of the critical stress intensity factor is related to the size of the active zone around the craze. The results presented in Table I suggest that in air and in benzene vapour the active zone is thicker than in the other environments investigated.

TABLE I Ratio of time to failure versus time to craze initiation, t_f/t_c, for PVC-CPE at 23 °C in some environments and the calculated critical stress intensity factors, K_{Ic} (Equation 16)

Environment	t_f/t_c	K_{Ic} (MPa $m^{1/2}$)	Failure
Air (g)	> 100	> 0.40	overall necking
Benzene (50% r. s.)	> 1000	> 0.50	local necking
n-Decane (50% r. s.)	100–300	0.40–0.45	brittle[a]
n-Octane (1)	100	0.40	brittle
n-Octane/benzene (90/10%) (1)	30	0.35	brittle
n-Octane/benzene (80/20%) (1)	30	0.35	brittle

[a] See Fig. 3.

6. Conclusions

The failure mechanisms observed in PVC and PVC-CPE for vapour and liquid environments start with craze initiation followed by a logarithmic craze growth process. The craze growth can cease by plastic deformation or plasticization of the polymer matrix around the craze. After the cessation of craze growth, the test strip will fail the moment the stress in the intact cross-section exceeds the drawing stress.

Continuous craze growth always leads to brittle failure. Continuous craze growth is stimulated by suppressing the plastic deformation around the craze. The brittle failure can be explained using a fracture mechanics criterion, namely a critical stress intensity factor. The test strips will show brittle failure by surface crazing after a surface craze reaches a size corresponding to the critical stress intensity factor.

The failure mechanisms considered in this paper will not occur below the craze initiation stress.

Acknowledgements

This work was sponsored by VEG-Gasinstituut, Nederlandse Gasunie and Ministerie van Economische Zaken. The author thanks Dr Ir. M. Wolters, Ir. L. Oranje, Dr P. Peereboom, Prof. Dr Ir. J. van Turnhout and Dr K. E. D. Wapenaar for valuable discussions and Mr A. M. Ringenaldus and Mr F. M. Dieleman for performing the experiments.

References

1. J. BREEN, *J. Mater. Sci.* **28** (1993) 3769.
2. J. BREEN and D. J. van DIJK, *ibid.* **26** (1991) 5212.
3. W. HASLETT and L. A. COHEN, *SPE J.* **20** (1964) 246.
4. M. E. R. SHANAHAN and J.SCHULTZ, *J. Polym. Sci. Polym. Phys.* **18** (1980) 1747.
5. M. K. V CHAN and J. G. WILLIAMS, *Polymer* **24** (1983) 234.
6. J. G. WILLIAMS and G. P. MARSHALL, *Proc. R. Soc. Lond. A* **342** (1975) 55.
7. R. J. FIELDS and M. F. ASHBY, *Phil. Mag.* **33** (1976) 33.
8. A. S. ARGON and M. SALAMA, *Mater. Sci. Engng* **23** (1976) 219.
9. Z. D. ZHANG, S. S. CHERN and C. C. CHSIAO, *J. Appl. Phys.* **54** (1983) 5568.
10. J. L. S. WALES, TNO memorandum 78/210 (1978).
11. N. VERHEULPEN-HEYMANS and J. C. BAUWENS, *J. Mater. Sci.* **11** (1976) 7.
12. H. H. KAUSCH, "Polymer Fracture", 2nd Edn (Springer, Berlin, 1987) p. 51.

13. F. GUIU and R. N. STEVENS, *J. Mater. Sci.* **26** (1991) 4375.
14. W. DÖLL and L. KÖNCZÖL, *Kunststoffe* **70** (1980) 563.
15. W. E. WARREN, A. CHUDNOVSKY and R. E. MULLEN, *Polym. Eng. Sci.* **29** (1989) 426.
16. D. BROEK, "Elementary engineering fracture mechanics", 4th Edn (Nijhoff, Dordecht, 1986) p. 75.
17. J. L. S. WALES, *Polymer* **21** (1980) 684.
18. H. R. BROWN, *J. Polym. Sci. Polym. Phys.* **27** (1989) 1273.

Received 29 April 1992
and accepted 24 February 1993